

Received January 31, 2018; reviewed; accepted April 25, 2018

Fluidization characteristics and separation performance of mild-hot gas-solid fluidized bed

Bo Lv^{1,2}, Zhenfu Luo^{1,2}, Bo Zhang^{1,2}, Yuemin Zhao^{1,2}, Yunfei Qin^{1,2}

¹ Key Laboratory of Coal Processing and Efficient Utilization of Ministry of Education, China University of Mining & Technology, Xuzhou 221116, China

² School of Chemical Engineering and Technology, China University of Mining and Technology, Xuzhou, 221116, China

Corresponding author: zfluo@cumt.edu.cn (Zhenfu Luo)

Abstract: In recent years, the mild-hot gas-solid fluidized bed had a crucial influence on wet-in-feed sorting when it comes to moist feed (e.g., lignite) because of its expanding sorting range. To explain the favorable sorting effect of the mild-hot gas-solid fluidized bed, the fluidization characteristics (e.g., the pressure drop, density, etc.) was studied under different work conditions. In addition, a high-speed dynamic camera was used in this study to compare the slumping behavior of the magnetite slag at different temperatures. The optimum conditions for coal separation was also studied by Design-Expert software. It was shown that the bed temperature of the fluidized bed has a particular effect on its stability when the bed temperature was below 120 °C, which had a great influence on the separation. Finally, the probable deviation E of the mild-hot gas-solid fluidized bed under optimum operation conditions could be as low as 0.09 g/cm³ which showed the good separation ability.

Keywords: dry coal separation, mild-hot gas-solid fluidized bed, bed temperature, fluidization characteristics

1. Introduction

The related instructions in the field of energy on the Chinese 13th Five-year Plan indicate that the high-efficiency clean coal resource utilization has become a trend (Ji et al., 2016; Huang et al., 2016; Zhang et al., 2015). Wet separation technology are universally used today for coal beneficiation both at home and abroad. These techniques are, however, unsuitable for coals located in water-deficient or in cold areas or for those coals that tend to slime in a wet separation process. In addition, a great deal of water is consumed and contaminated during the wet separation. Water is, however, valuable all around the world today. Therefore, the dry separation technology without water is an effective method of solving the abovementioned problems. Gas-solid fluidization technology was first applied to coal separation as early as the 1920s. There after a number of scientists and engineers in many countries contributed to the development of dry coal-cleaning using gas-solid fluidized beds (Chalavadi et al., 2015; Lu et al., 2003; Zhao et al., 2014; Luo et al., 2013; Chen et al., 2015).

The gas-solid fluidized bed with an obvious separation effect and a relatively mature technology presently occupies an important position in the technical field of dry sorting (Weitkaemper and Wotruba, 2010; Oshitani et al., 2016; He et al., 2016; Wang et al., 2016). The bed temperature has an important influence on the wet feeding separation because the separation range of the gas-solid fluidized bed has expanded in the recent years, particularly in relation to the wet feed, such as lignite (Chu and Li, 2005; Zhao et al., 2015). However, only a few studies focused on the effect of the bed temperature on the fluidization characteristics. Accordingly, Lettieri et al. (2001) showed that the surface characteristics and many fundamental characteristics of the dense phase would change with the increasing bed operating temperature in the fluidized bed. Choi et al. (2003) reported that the qualitative change in the minimum slugging velocity agreed with the inverse of the minimum fluidizing velocity

as the temperature was varied. The slug frequency slightly decreased, whereas the slug rising velocity increased as the bed temperature increased. Girimonte et al. (2014) and Formisani et al. (2002) found that the temperature rise would cause the bubble size to decrease. However, their research was confined to the fundamental characteristics of the gas fluidized bed. Therefore, studying the effect of the bed temperature on the fluidization characteristics of the gas–solid fluidized bed is very important.

2. Experimental

2.1. Experimental apparatus and material

The experimental apparatus in Fig. 1 was used to study the fluidization characteristics and separation performance of mild-hot gas-solid fluidized bed. The bed body in the fluidized bed model, which was made of organic glass, was a rectangular structure measuring 300 mm × 200 mm × 500 mm. The system was mainly composed of a blower; an air heater; a temperature control device; a micro-differential pressure transformer; a gas rotameter; and a fluidized bed comprising the upper election room, air distribution plate, and lower wind chamber. As for the fluidized bed structure, the upper election room was processed by the organic glass to observe the fluidized state of the particles in the bed. The air distribution plate adopted the organic glass plate and the double-layer porous cloth bolted together. The lower air chamber was welded by a steel plate. For research convenience, the high-speed dynamic camera was installed on the side of the bed body, which can be used to calibrate the heights change of the fluidized bed and the sample. An intrusive pressure measurement probe was also prepared to measure the internal pressure drop. For measuring the bed density, the fluidized bed was divided into three regions, labeled as L1 (40 ~ 60mm), L2 (80 ~ 100mm) and L3 (120 ~ 140mm), the cross section of each region had five measuring points (the left of the two measuring points, the middle of a measuring point, the right of the two test points).

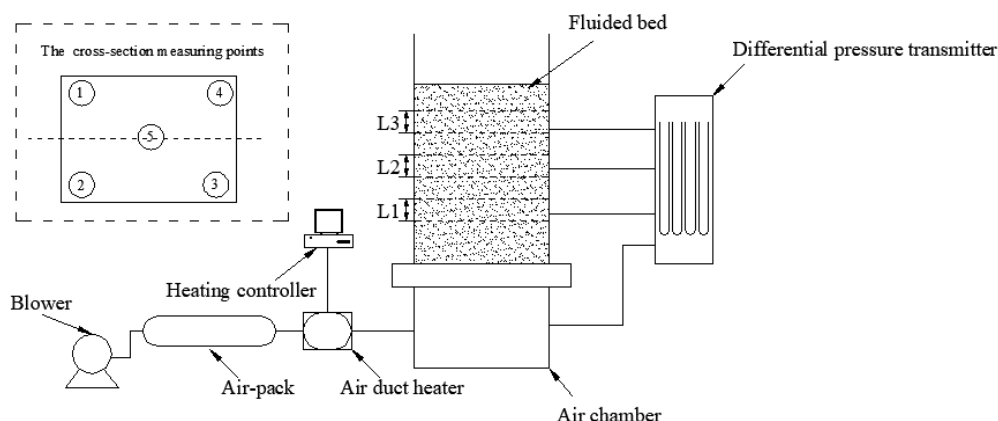


Fig. 1. Schematic diagram of the experimental apparatus

An air duct heater was utilized to heat the fluidized gas and achieve a different bed temperature. A PXR5TEY1-8W000-C type heating controller was also employed to stabilize the bed temperature fluctuation.

Table 1 Granularity of the media

Size(mm)	Fraction content (%)
+0.3	0.7
0.3 ~ 0.15	68.9
0.15 ~ 0.074	29
-0.074	1.4
Total	100.0

The gas pressure was controlled at approximately 0.02 MPa. The heavy particle was made by a wide particle grade and a high-density magnetite. The true density was 4200 kg/m³. The magnetic material content was 99.71%, while the magnetization was 77.21 emu/g. Table 1 shows the grain size composition.

2.2. Evaluation

An important index of the fluidization stability of mild-hot gas–solid separation fluidized beds is the density fluctuation variance S_p , given as follows:

$$S_p = \sqrt{\frac{\sum_i^n (\rho - \rho_0)^2}{n}} \quad (1)$$

where ρ is the local bed density (cm/s); ρ_0 is the average density (cm/s); and n is the number of measurements.

Furthermore, the slumping behavior of the fluidized bed was compared as follows by introducing the standard collapse time (SCT) using Eq. (2):

$$SCT = \frac{t_s - t_o}{H_s} \times 100 \quad (2)$$

where H_s is the static bed height after slumping (mm); t_o is the start time for slumping behavior(s); and t_s is the end time for slumping behavior(s).

3. Bed temperature implementation

Two methods are presently utilized to regulate the mild-hot gas–solid fluidized bed. The first one is to adjust the surface temperature of the fluidized medium. The second one is to regulate the fluidized gas temperature (Nemati et al., 2016; Mohammad and Jamal, 2015). As shown in Fig. 2a, the former method needed a preheated convection medium (i.e., magnetite). However, in the continuous flow process, the preheated medium will continue to reduce the surface temperature to room temperature. A circulation heating device must be increased to maintain the fluidizing medium surface temperature, which will not only result in the increase of the operating cost, but will also reduce the stability of the fluidized bed. The latter method only requires adding a set of heaters in the fluidized gas pipeline in Fig. 2b. The temperature distribution on the cross section in the early fluidizing stage of the bed is uneven, which showed a high phenomenon on the bottom. However, the difference will be very small in the final normal flow process and can be ignored.

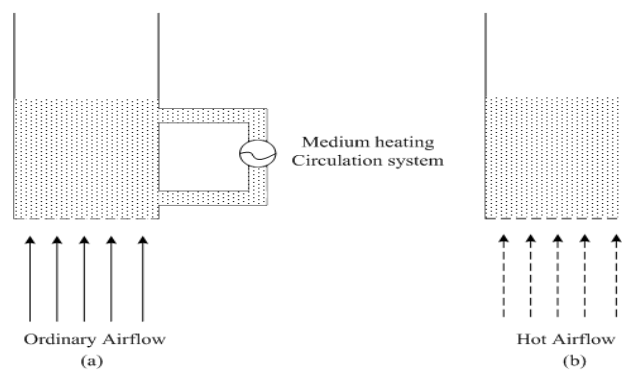


Fig. 2. Bed temperature implementation.

The mild-hot gas–solid fluidized bed is very favorable for the wet mineral separation. More surface moisture adhesions become a part of the fluidized media when the wet mineral is sorted, thereby resulting in the loss of the streaming media. However, these adhesions will increase the moisture content of the fluidized bed and improve its viscosity, which results in the eventual deterioration of the environment (He et al., 2015; Fan and Dong, 2015; Qian et al., 1996). At this point, the mild-hot gas–solids fluidized bed can accelerate the surface water evaporation to dry the wet mineral. At the same time, the water content in the fluidized bed can be reduced to prevent the flow of the media into a mass,

thereby improving the flow of the bed environment. However, many problems still need to be studied and resolved.

4. Results and discussion

4.1. The pressure drop state

The fluidized state of the mild-hot gas-solid fluidized bed was mainly reflected in the pressure drop change of the bed layer, which visually represented the bed from the fixed to the fluidized. Fig. 3a shows the fluidization characteristic curve under various conditions. The curve analysis showed that the fluidization curves gradually shifted to the left and the pressure drop of the bed layer after being fluidized consistently stabilized with the bed temperature increase. The pressure drop of the ordinary gas-solid bed had difficulty in remaining stable after reaching a critical fluidized gas velocity. In contrast, the pressure drop of the mild-hot fluidized bed can remain conversely stable. And the critical fluidized gas velocity decreased with the increase of temperature which showed that the bed temperature may enhance fluidization. Relatively, when the bed temperature was very high (e.g.160 °C), the fluctuation of bed layer is larger shown as Fig. 3b.

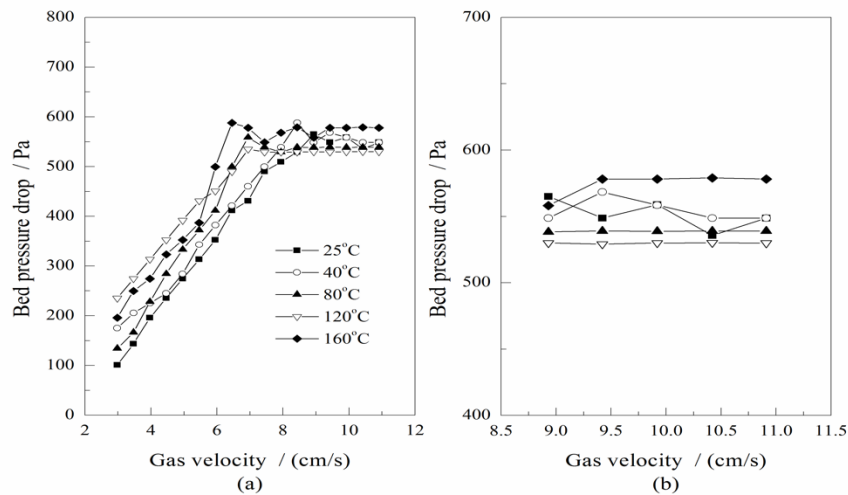


Fig. 3. Comparison of bed pressure drops at different temperatures.

Table 2 shows that the pressure drop fluctuation variance of the ordinary fluidized bed was 0.1108. The variance was reduced to 0.0053 with the hot air flow, which was sufficient to show that the stability of the mild-hot fluidized bed improved. However, the bed pressure drop variation was large, and the bed stability decreased when the bed temperature reached 160 °C. As has been known from the analysis, the fluidized gas viscosity was too large; the density decreased; and the gas volume stability was poor in an ultra-high bed temperature. The abovementioned findings showed that forming a stable bubble flow was difficult even in the case of a constant flow rate. Accordingly, the bed temperature should be controlled in a proper range to reduce the pressure drop fluctuation and improve the stability of the mild-hot fluidized bed in the actual production.

Table 2 Fluctuation variance of bed pressure drop after stable fluidization

Gas velocity (cm/s)	Bed pressure drop (KPa)				
	25°C	40°C	80°C	120°C	160°C
8.93	0.565	0.549	0.538	0.530	0.558
9.92	0.559	0.559	0.539	0.530	0.578
10.91	0.549	0.549	0.539	0.530	0.578
Average value	0.552	0.555	0.537	0.530	0.572
σ	0.1108	0.0856	0.0374	0.0053	0.1108

4.2. The bed density state

The axial pressure drop on the bed side and the central position were measured by the intrusive pressure measurement probe under different bed temperatures. The values were then converted into the bed density variance shown in Fig. 4. Overall, the temperature increase can play a role in the relaxation of the bed's axial density fluctuation. The maximum density variance on the left side of the fluidized bed was reduced along with the bed temperature increase. The value can be reduced to 0.15 g/cm³ when the temperature reaches 120 °C. The stratification phenomenon of the axial density then disappears. The analysis showed that the gas viscosity increased with the bed temperature increase, and the gas fully contacted with the medium particles. On the other hand, the motion of the medium particles is more active in the high temperature environment. In result, the gas-solid phase was relatively uniform. However, the maximum density difference of the bed layer improved when the temperature further increased. For explaining the above phenomenon, the formed bubble assumed some negative functions under high temperatures. According to the Davidson bubble model, the bubble formed without particles was considered as a sphere. Its average size was larger as the temperature increased to aggravate the bubbling and the medium back-mixing in the fluidized bed. As a result, the density fluctuation of the bed layer became larger. The experimental data showed a different change in the trends in the right, which can possibly be caused by the uneven flow gas distribution. However, overall, the proper temperature can play an active role in regulating the axial flow density.

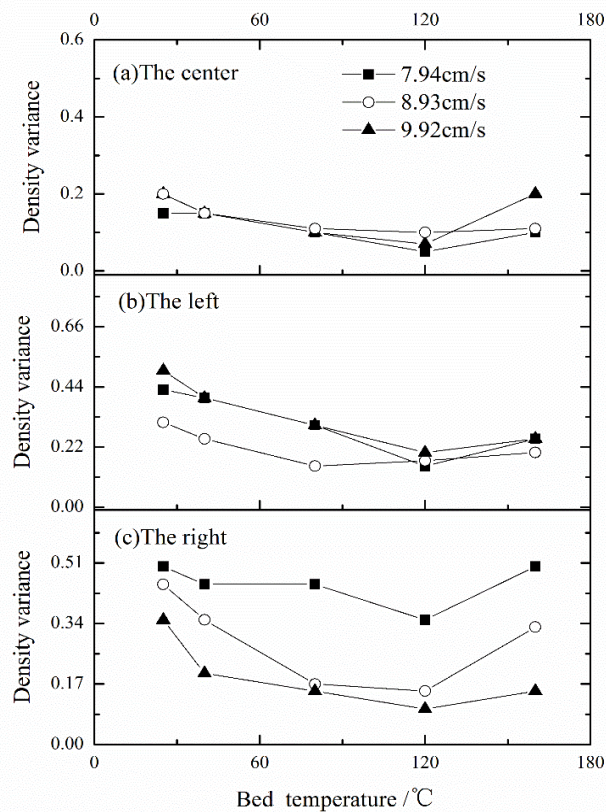


Fig. 4. The axial bed density variance

Fig. 4 showed that the center flow density difference must be less than the side. Furthermore, the density distribution was relatively uniform whenever under ambient temperature or a hot condition because the influence of the side wall effect caused the partial dead zone in the corner, which led to the decrease of the bed stability.

After accumulating enough data, we calculated the determination of the radial flow density within different bed temperature. Using Gaussian model after ignoring the effect of bed height, we fitted the above data curve such as Eq. (3). In the formula, S_p was the density variance value, t was the bed temperature, y_0 , a , t_c , w and p_i were constant which was shown in the following table3, so the density variance value and bed temperature were inversely proportional within a certain range.

$$S_p = y_0 + \frac{a}{w \times e^{2 \times \left(\frac{t-t_c}{2}\right)^2} \times \sqrt{\frac{p_i}{2}}} \quad (3)$$

Table 3 Value of the constant in Eq. (3)

Gas velocity (cm/s)	constant	value	Reduced Chi-Sqr	Fit status
7.94	y ₀	5.5864	0.00212	Succeeded
	a	-4927.67		
	t _c	107.09		
	w	727.023		
8.93	y ₀	17.0345	0.00294	Succeeded
	a	-29628.34		
	t _c	115.738		
	w	1399.47		
9.92	y ₀	34.49	0.00384	Succeeded
	a	-66463.09		
	t _c	106.34		
	w	1541.46		

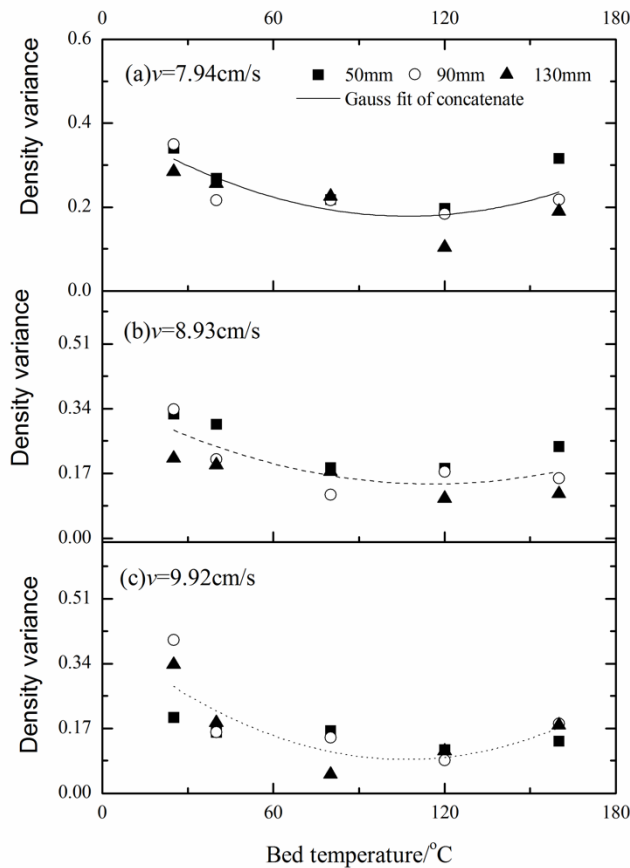


Fig. 5. Fitting curve of the radial bed density variance value

The determination of the radial flow density within different bed heights (Fig. 5) showed that the radial density difference first decreased and then increased with the bed temperature increment. Overall, the variance curve of the density fluctuation once fell to a low point when the bed temperature was from 80 to 120 °C, and the radial flow density relatively changed the alleviation. The analysis further showed that the gas–solid fluidized bed was considered as a macroscopic whole if a single heavy particle was considered as a microscopic individual. On the micro level, every heavy particle is

suspended similar to the unstable state of the Brownian particle at the effect of bubble, drag, and pressure gradient forces. This effect gradually improves with the bed temperature increase to promote medium mixing and enhance the radial density uniformity. Meanwhile, the medium mixing phenomenon was obvious, which affected the distribution of the particles at the macro level. However, the mixing phenomenon was stronger when the bed temperature exceeded this range, especially after the temperature reaches 160 °C. The flow state also became worse in conspiring against the separation. This result might have been caused by the new unstable factors that the high temperature produced or by the bubble size that increased with the increasing temperature. The gas viscosity also increased, which caused the channeling phenomenon in local area. Therefore, the bed temperature must be controlled within a reasonable range to ensure the stability of the fluidized bed. Additionally, the variance value of the bed density decreased with the increase of the gas velocity by the comparison of three fitting curves from Fig. 6, illustrating that the gas velocity has a certain influence on the fluidization characteristics of the bed layer, and then validating the previous research results.

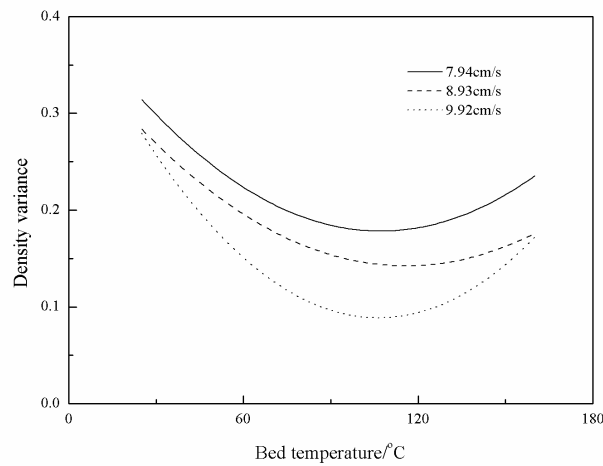


Fig. 6. Comparison of three fitting curves

4.3. The bed collapse behavior

The bed collapse behavior was another manifestation of the bed's fluidization behavior. The collapse process of the mild-hot gas-solid fluidized bed was recorded using a high-speed dynamic camera (Fig. 7). A collapse curve was obtained (Fig. 8a) after the treatment. At the same time, the collapse curve of this group was also analyzed.

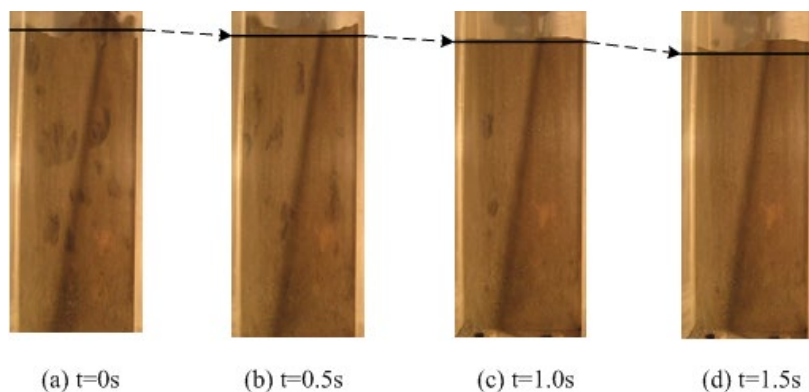


Fig. 7. High-speed photographic images of the collapse process

Fig. 8b shows the SCT value of the magnetite slumping process illustrating a clear upward trend with the bed temperature increase. The findings indirectly confirmed that increasing the bed temperature helped improve the gas detention ability of the particles in the fluidized bed. This result has a positive effect on improving the fluidization characteristics of the fluidized bed.

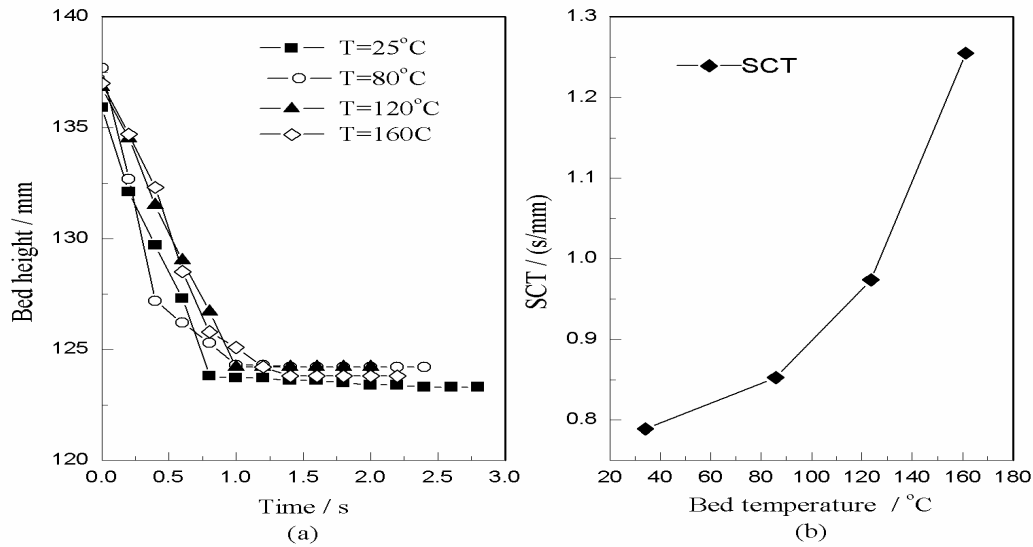


Fig. 8. Bed collapse curve with the bed temperature increase

4.4. Analysis of orthogonal experiment results

According to the analysis of above data in the study, bed temperature and fluidized gas velocity had a certain interaction on the fluidization characteristics of the fluidized bed for the final separation performance. In order to facilitate numerical analysis, the density distribution was used to estimate the fluidization characteristics for separation. The results were analyzed from two-factor and four-level orthogonal test in Table 4 by Design-Expert software.

Table 4. Experimental design and results

S _{td}	Run	Factor 1	Factor 2	Response 1
		A bed temperature (°C)	B Gas velocity (cm/s)	The standard deviation of the density distribution (g/cm ³)
10	1	80.00	9.92	0.14725
13	2	40.00	10.91	0.18823
6	3	80.00	8.93	0.20200
14	4	80.00	10.91	0.14514
9	5	40.00	9.92	0.19852
5	6	40.00	8.93	0.23107
4	7	160.00	7.94	0.11326
11	8	120.00	9.92	0.09220
8	9	160.00	8.93	0.15200
2	10	80.00	7.94	0.12334
1	11	40.00	7.94	0.18066
16	12	160.00	10.91	0.13312
7	13	120.00	8.93	0.17573
15	14	120.00	10.91	0.11370
12	15	160.00	9.92	0.13222
3	16	120.00	7.94	0.04952

The standard deviation of Cubic model was the smallest and the variance of the model was 0.924, so it was suitable for the analysis of the experiment results. On the basis of the model, the coefficients of each factor in the model were estimated.

Through the above analysis, the fitting model describing the standard deviation of the density distribution and the parameters was obtained:

$$S_p = -25.61425 + 1.50773E - 3T + 8.16376V - 1.91475E - 4YV - 3.27121E - 5T^2 - 0.85296V^2 - 1.41586E - 6T^2V + 2.84933E - 5V^2 + 1.9E - 7T^2 \quad (4)$$

In Eq. (4), S_p was the standard deviation of the density distribution, T was bed temperature and V was gas velocity. The comparison of predicted and experimental value of S_p were sew as Fig. 9. It could be seen that the linear distribution of the residual data was obvious, which proved that the model could well fit the experimental data. The comparison of predicted and experimental values was almost in a straight line indicating a good consistency between the two.

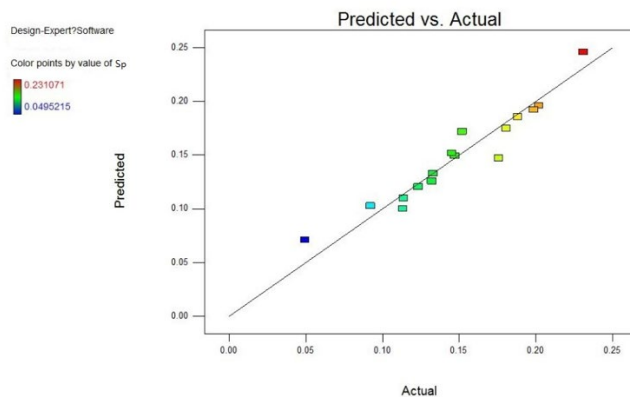


Fig. 9. Predicted vs. experimental value of S_p

The response surface for the effects of the above factors on the density distribution is shown in Fig. 10 and Fig. 11. In addition, the contours for different operating conditions are shown. The peak segregation intensity is achieved when the bed temperature are roughly 120°C for the low density distribution. The effect of the bed temperature the segregation intensity is more sensitive than that of gas velocity.

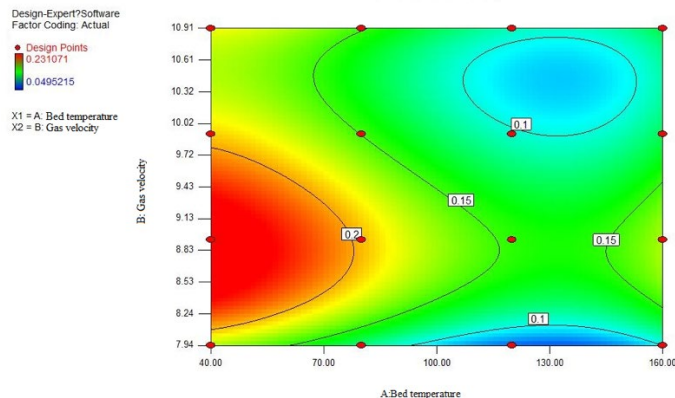


Fig. 10. Contour map of density distribution standard deviation

From the above orthogonal test, the influence factors of the standard deviation S_p of the bed density distribution were optimized by the software, and the optimization scheme was given, as shown in Table 5 which was expected that the bed would show good fluidization state under the optimized condition and then provide a good environment for coal separation.

Table 5. Optimization schemes of S_p value

Run	Bed temperature (°C)	Gas velocity (cm/s)	The standard deviation of the density distribution (g/cm ³)	Credibility value
1	120.22	7.94	0.0682636	0.705
2	121.85	10.41	0.0857393	0.629

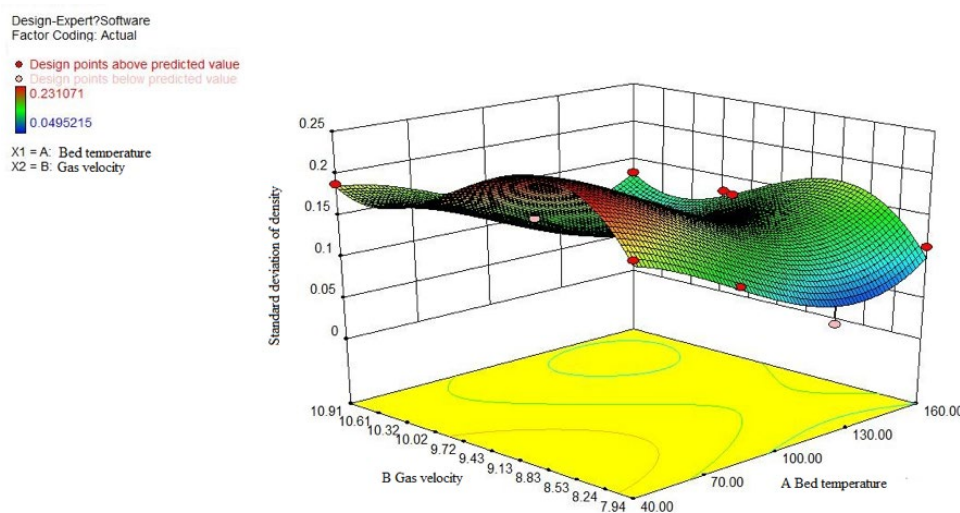


Fig. 11. 3D response surface of S_p value and various factors

4.5. Separation efficiency

Under the optimum conditions, the value first decreased and then increased with the bed temperature increase. The possible deviation of the mild-hot gas–solid separation fluidized can be lower under the optimum conditions of 121°C and 10.41 cm/s. Therefore, the separation experiment of raw coal should be carried out under this condition.

Table 6. Partition coefficient of the separation

Density rang(g/cm ³)	Clean coal product (%)			Gangue product (%)			Calculated feedstock (%)		Partition coefficient (%)
	O	O/F	Ash	O	O/F	Ash	F	Ash	
-1.4	29.38	12.49	6.82	0.59	0.34	7.40	12.83	6.84	2.65
1.4-1.5	50.22	21.34	11.01	2.42	1.39	11.42	22.73	11.04	6.12
1.5-1.6	9.3	3.95	20.52	0.5	0.29	29.25	4.24	21.12	6.84
1.6-1.8	10.13	4.3	32.12	1.05	0.61	38.12	4.91	32.87	12.42
1.8-2.0	0.67	0.28	45.53	7.44	4.28	41.52	4.56	41.77	93.86
2	0.3	0.13	50.10	88	50.6	62.12	50.73	62.09	99.74
Total	100	42.49	9.21	100	57.51	55.59	100	35.88	

O = Weight fraction, O/F = Yield, F = Weight fraction

In the field of coal beneficiation, the separation performance is commonly evaluated by the probable error E which is obtained from the partition curve of coal separation. And the experimental data used to plot the partition curve is derived from the float-and-sink analysis of the products. The separation experiment of raw coal is carried out in the mild-hot gas-solid fluidized bed and the stratified particulate bed is divided evenly into four layers. Coal particles in the top two layers are collected after screening, acting as the clean coal product. Likewise, coal particles in the bottom layer are handled as the gangue product. The results of float-and-sink and ash analysis of these two products are given in Table 6. When the separating density was 1.79 g/cm³, the ash content was reduced from 35.88% in the feedstock to 9.21% in the separated product. The clean coal recovery was 42.49% and the probable error, E , value was 0.090 g/cm³, which indicate the good separation ability of the mild-hot gas-solid fluidized bed as shown in Fig. 12.

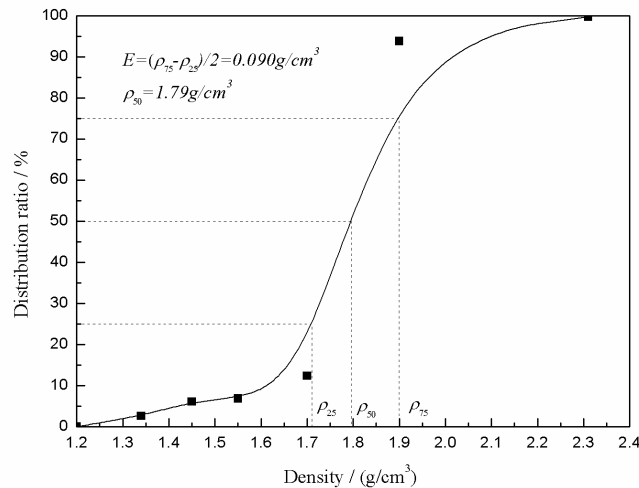


Fig. 12. Distribute cure as the separation in the experiment

5. Conclusions

The following conclusions are drawn from this study:

(1) The bed temperature within the appropriate range helps improve the fluidization characteristics of the mild-hot gas–solid fluidized beds. The study shows that the fluctuation range of the pressure drop and the flow density decrease with the bed temperature increase below 160 °C. Furthermore, the standard slump time of the fluidized bed increases to improve the gas detention ability of the particles. However, up to 160 °C, the fluidized gas viscosity is too large, the density decreases, and the gas volume stability is too poor to form a stable bubble flow even in the case of a constant flow rate. Accordingly, the bed temperature should be controlled in a proper range to reduce the pressure drop fluctuation and improve the stability of the fluidized bed in the actual production.

(2) According to the analysis of above data in the study, bed temperature and fluidized gas velocity have a certain interaction on the bed density distribution. By Design-Expert software, we can obtain the mathematical model describing the standard deviation of the density distribution and the above parameters and receive the optimum conditions of the mild-hot gas–solid fluidized beds for coal separation.

(3) The mild-hot gas–solid fluidized bed has a particular the separation efficiency. In the actual sorting process, the possible deviation E is affected by the temperature. The value first decreases and then increases, especially at approximately 120 °C, as the temperature increases. The probable error, E , value was 0.090 g/cm³, which indicates that the good separation efficiency of the mild-hot gas–solid fluidized bed in the optimum temperature range.

Acknowledgments

The authors acknowledge the financial support by the National Natural Science Foundation of China (No. 51774283), the Fundamental Research Funds for the Central Universities(2018BSCXB08), the Postgraduate Research & Practice Innovation Program of Jiangsu Province, and the Fundamental Research Funds for the Central Universities(2018XKQYMS05).

References

- CHALAYADI, G., SINGH, R. K., SHARMA, M., SINGH, R., DAS, A., 2015. *Development of a Generalized Strategy for Dry Beneficiation of Fine Coal over a Vibrating Inclined Deck*. International Journal of Coal Preparation and Utilization. 36(1): 10-27.
- CHEN, J., SHEN, L., LIU, C., SUI, Z., 2015. *Study of motion characteristics of the vibrated spiral dry separator*. Journal of China University of Mining & Technology. 44(1):125-131.
- CHOI, J.H., KIMA, T.W., MOON, Y.S., KIM, S.D., SON, J.E., 2003. *Effect of temperature on slug properties in a gas fluidized bed*. Powder Technology. 131: 15-22.

- CHU, M., LI, H.M., 2005. *The processing and utilization technology of lignite coal*. Coal Engineering. (2): 47-49.
- FAN, Y.P., DONG, X.S., 2015. *Synergistic effects of ultrasound and electrolysis on the dehydration of fine lignite coal*. Energy Technology. 3(11):1084-1092.
- FORMISANI, B., GIRIMONTE, R., PATARO, G., 2002. *The influence of operating temperature on the dense phase properties of bubbling fluidized beds of solids*. Powder Technology. 125(1):28-38.
- GIRIMONTE, R., FORMISANI, B., 2014. *Effects of operating temperature on the bubble phase properties in fluidized beds of FCC particles*. Powder Technology, 262(2):14-21.
- HE, J.F., ZHAO, Y.M., ZHAO, J., LUO, Z.F., DUAN, C.L., HE, Y.Q., 2015. *Enhancing fluidization stability and improving separation performance of fine lignite with vibrated gas-solid fluidized bed*. Canadian Journal of Chemical Engineering. 93(10):1793-1801.
- HE, Y.Q., TAN, M.B., ZHU, R., DUAN, C.L., 2016. *Process optimization for coal cleaning by enhancing the air-distribution stability of dry separator*. Powder Technology. 288: 45-54.
- HUANG, B., ZHAO, X., ZHANG, Q., 2016. *Framework of the theory and technology for simultaneous mining of coal and its associated resources*. Journal of China University of Mining & Technology. 45(4):653-662.
- JI, Y.L., REN, T., WYNNE, P., WAN, Z.J., MA, Z.Y., WANG, Z.M., 2016. *A comparative study of dust control practices in Chinese and Australian longwall coal mines*. International Journal of Mining Science and Technology. 26(2):199-208.
- LETTIERI, P., NEWTON, D., YATES, J.G., 2001. *High temperature effects on the dense phase properties of gas fluidized beds*. Powder Technology. 12:34-40.
- LU, M., YANG, Y., LI, G., 2003. *The application of compound dry separation in China*. In Proceedings of 20th International Coal Preparation Conference. 81-95.
- LUO, Z.F., ZHAO, Y.M., TAO, X.X., FAN, M.M., CHEN, Q.R., 2003. *Progress in Dry Coal Cleaning Using Air-Dense Medium Fluidized Beds*. Coal Preparation. 23(1-2): 13-20.
- MOHAMMED, L., JAMAL, C., 2015. *A novel induction heating fluidized bed reactor: Its design and applications in high temperature screening tests with solid feedstocks and prediction of defluidization state*. American Institute of Chemical Engineers. 61(5): 1507-1523.
- NEMATI, N., ZARGHAMI, R., MOSTOUFI, N., 2016. *Investigation of hydrodynamics of high-temperature fluidized beds by pressure fluctuations*. Chemical Engineering & Technology. 39(8): 1527-1536.
- OSHITANI, J., TERAMOTO, K., YOSHIDA, M., KUBO, Y., NAKATSUKASA, K., 2016. *Dry beneficiation of fine coal using density-segregation in a gas-solid fluidized bed*. Advanced Powder Technology. 27(4):1689-1693.
- QIAN, S.Z., LU, J.D., 1996. *Critical fluidization behavior of high temperature gas-solid fluidized bed*. Combustion Science and Technology. 2 (4): 315-321.
- WANG, Y.N., LUO, Z.F., HUANG, G., REN, B.J., 2016. *Effect of agitation on the characteristics of air dense medium fluidization*. International Journal of Mining Science and Technology. 26(3), 383-387.
- WEITKAEMPER, L., WOTRUBA, H., 2010. *Effective dry density beneficiation of fine coal using a new developed fluidized bed separator*. Proceedings of the International Coal Preparation Congress, Australia, F.
- ZHANG, B., ZHAO, Y.M., ZHOU, C., DUAN, C., DONG, L., 2015. *Fine coal desulfurization by magnetic separation and the behavior of sulfur component response in microwave energy pretreatment*. Energy Fuels. 29(2):1243-1248.
- ZHAO, P.F., ZHAO, Y.M., CHEN, Z.Q., LUO, Z.F., 2015. *Dry cleaning of fine lignite in a vibrated gas-fluidized bed: Segregation characteristics*. Fuel. 142:274-282.
- ZHAO, Y.M., YANG, X.L., LUO, Z.F., DUAN, C.L., SONG, S.L., 2014. *Progress in developments of dry coal beneficiation*. International Journal of Coal Science & Technology. 1(1): 103-112.